


RESEARCH ARTICLE | JUNE 01 2023

Revisiting thermal transport in single-layer graphene: On the applicability of thermal snapshot interatomic force constant extraction methodology for layered materials

Shadab Alam ; Amey G. Gokhale ; Ankit Jain 



Journal of Applied Physics 133, 215102 (2023)

<https://doi.org/10.1063/5.0152112>



CrossMark

Articles You May Be Interested In

Bandgap formation mechanisms in periodic materials and structures

Proc. Mtgs. Acoust (June 2013)

Electronic and magnetic properties of Si substituted Fe₃Ge

Journal of Applied Physics (September 2015)

Investigations on the structural, multiferroic, and magnetoelectric properties of Ba_{1-x}Ce_xTiO₃ particles

Journal of Applied Physics (June 2018)

AIP Advances

Why Publish With Us?

	25 DAYS average time to 1st decision		740+ DOWNLOADS average per article		INCLUSIVE scope
---	--	---	--	---	---------------------------

[Learn More](#)



Revisiting thermal transport in single-layer graphene: On the applicability of thermal snapshot interatomic force constant extraction methodology for layered materials

Cite as: J. Appl. Phys. **133**, 215102 (2023); doi: [10.1063/5.0152112](https://doi.org/10.1063/5.0152112)

Submitted: 28 March 2023 · Accepted: 11 May 2023 ·

Published Online: 1 June 2023



View Online



Export Citation



CrossMark

Shadab Alam,  Amey G. Gokhale,  and Ankit Jain^{a)} 

AFFILIATIONS

Mechanical Engineering Department, IIT Bombay, Mumbai, Maharashtra 400076, India

^{a)}Author to whom correspondence should be addressed: a_jain@iitb.ac.in

ABSTRACT

The thermal conductivities of single-/bi-layer graphene and bulk-graphite are obtained using the Boltzmann transport equation (BTE) framework by accounting for three-phonon and four-phonon scatterings. For single-layer graphene, the thermal conductivity and interatomic force constants obtained using temperature-independent finite-difference, and temperature-dependent molecular dynamics-based approaches agree with each other. The use of the thermal snapshot approach to get temperature-dependent force constants results in a non-physical description of interatomic distances for single-layer graphene. The predicted thermal conductivity at room temperature using finite-difference based force constants is 800 W/m K, which is a severe under-prediction of experimentally measured values. For bi-layer graphene and bulk graphite, the thermal snapshot methodology is applicable and thermal conductivity changes by 25% and 5% with temperature-dependent force constants. The effect of four-phonon scattering is less than 10% on the predicted thermal conductivity of bi-layer graphene and graphite, and the obtained thermal conductivities using thermal snapshot methodology are in agreement with the literature. The limitation in the prediction of thermal conductivity of single-layer graphene via the BTE approach stems from non-accountability of temperature-dependence in finite-difference based force constants and non-physical description of interatomic bonds in thermal snapshot based force constants extraction for planar 2-atoms unitcell of single layer graphene.

Published under an exclusive license by AIP Publishing. <https://doi.org/10.1063/5.0152112>

I. INTRODUCTION

Graphene has the highest thermal conductivity among all materials with measured room temperature values of 1500–5000 W/m K^{1–3} for freely suspended samples, 600 W/m K for supported samples,⁴ and 2200–4400 W/m K for isotopically modified samples.⁵ Along with challenges in experimental measurements, this large spread in measured thermal conductivity depending on the sample size, support, defect, etc. (along with high reported values in the range of 1500–5000 W/m K) suggests weak intrinsic heat carrier (phonon) scattering. Earlier atomistic calculations based on the iterative solution of the Boltzmann transport equation (BTE) supported these findings, and phonon–boundary scattering was found necessary to obtain the converged thermal conductivity for freely suspended graphene.^{6,7} In particular, calculations suggested the

non-scattering of flexural acoustic phonons via three-phonon processes owing to out-of-plane crystal symmetry.⁶ With advances in computations, which now allow for the possibility of including four-phonon scattering processes,^{8–11} however, this original understanding is challenged and flexural modes are found to undergo scattering along with an accompanied fourfold decrease in the predicted thermal conductivity (and therefore, under-prediction of the experimentally measured values by a factor of 4–5).¹²

Additionally, the predicted thermal conductivity from the BTE-based approach with four-phonon scattering also falls short of that obtained from classical molecular dynamics simulations, even after accounting for quantum corrections and employing the same interatomic force field.^{12,13} Analysis by Gu *et al.* suggested that this under-prediction of thermal conductivity with the inclusion of

four-phonon scattering in the BTE approach is due to the use of zero temperature sampling of the potential energy surface (based on finite-difference based force constants) and with temperature-dependent force constants (using the stochastic thermal snapshot technique¹⁴), the thermal conductivity increases by 50%.¹³ The strong temperature-dependence of interatomic interactions in graphene at room temperature is puzzling as, on the one hand, graphene has strong carbon-carbon sp^2 bonds with an extremely high Debye temperature of ~ 2000 K,¹⁵ and on the other hand, the freely suspended graphene is debated to have large ripples arising from thermal fluctuations,¹⁶ potentially resulting in large atomic displacements (and hence, strong temperature-dependence of the potential energy surface). In the latter case, however, the validity of the available force constants extraction methodology (via the Taylor-series fit to force-displacement data around periodic equilibrium atomic positions) is questionable.

There is, therefore, a need to re-examine the validity of interatomic force constants in describing the thermal transport properties of freely suspended graphene and layered materials.

In this work, we revisited different interatomic force constants extraction methodologies for the BTE-based thermal conductivity prediction of graphene. We use the (i) finite-difference (temperature-independent), (ii) thermal snapshot (temperature-dependent), and (iii) molecular dynamics (temperature-dependent) driven force constants. We considered both three-phonon and four-phonon scatterings and investigated thermal transport in single-bi-layer graphene and bulk graphite. We find that for single-layer graphene, the force constants and thermal conductivities obtained from finite-difference and molecular dynamics-based approaches are in perfect agreement with each other. However, since the computational cell employed for force constants extraction is relatively small in molecular dynamics simulations, the obtained thermally perturbed graphene structures are ripple-free. On the other hand, with the thermal snapshot technique, while the structural ripples are captured even with relatively small computational cells, the obtained thermal displacements are more than 2–3 Å in the cross-plane direction, thus limiting the use of Taylor-series fitting for force constant extraction and destroying the lattice periodicity. Furthermore, due to the decoupling of flexural and basal-plane modes in single-layer graphene, these large cross-plane displacements get manifested in erroneously large bond lengths ranging up to 2.5 Å (compared to equilibrium bond length of 1.45 Å). These non-physical bond lengths are present only in single-layer graphene and with the introduction of another layer in bi-layer graphene, all obtained bond lengths are less than 1.6 Å using the thermal snapshot methodology.

In the following, we start with thermal transport methodology and discuss different interatomic force constants extraction methodologies in Sec. II and related computational details in Sec. III. In Sec. IV, we start with the results for thermal transport in single-layer graphene using the relaxation time approximation of the BTE and discuss the effect of different force constant extraction methodologies on the predicted thermal conductivity. Later, we include results using the iterative solution of the BTE for all three of single-/bi-layer graphene and bulk graphite. In Secs. V and VI, we end by presenting our takeaway conclusions from this study.

II. METHODOLOGY

While the full details regarding the calculation of thermal conductivity from BTE can be found elsewhere,^{8,17} the thermal conductivity, k_{ph} , is obtained as

$$k_{ph}^{\alpha} = \sum_i c_{ph,i} v_{\alpha}^2 \tau_i^{\alpha}, \quad (1)$$

where the summation is over all the phonon modes in the Brillouin zone enumerated by $i \equiv (q, \nu)$, where q and ν are phonon wavevector and mode index, and $c_{ph,i}$, v_{α} , and τ_i^{α} represent phonon specific heat, group velocity (α -component), and transport lifetime, respectively. The transport lifetimes are obtained by considering phonon-phonon scattering via three- and four-phonon scattering processes and phonon-boundary scattering corresponding to a characteristic length scale, L_{bdry} , of $9 \mu\text{m}$, i.e., $1/\tau_{bdry} = L_{bdry}/|v|$.

The computation of phonon mode properties (heat capacity, group velocity, three-phonon, and four-phonon scattering rates) requires harmonic, cubic, and quartic interatomic force constants.⁸ For stiff materials with high Debye temperature, these required interatomic force constants can be obtained from finite-difference of forces obtained by displacing one or more atoms from their equilibrium positions. The force constants obtained using this approach [labeled as finite-difference (FD)] correspond to the equilibrium positions of atoms and do not account for temperature dependence arising from the thermal perturbations of atoms.

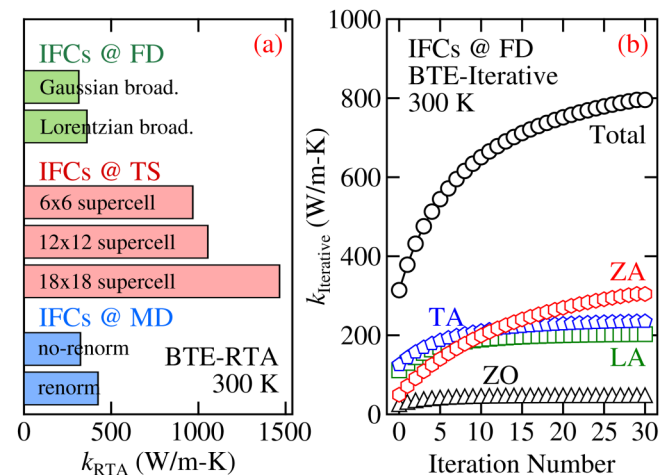


FIG. 1. The BTE predicted thermal conductivity of single-layer graphene as obtained using (a) RTA approximation with IFCs obtained from finite-difference (FD), thermal snapshot (TS), and molecular dynamics (MD) approaches, and (b) iterative/full solution with IFCs from the FD approach. The effect of broadening and renormalization is presented in (a) for FD- and MD-based IFCs. All thermal conductivities are obtained at 300 K using optimized Tersoff interatomic interactions by accounting for three-phonon and four-phonon scatterings for a sample size of $9 \mu\text{m}$.

Alternatively, the atoms can be thermally perturbed in computational cells according to^{14,18,19}

$$u_{b,l}^\alpha = \frac{1}{\sqrt{N}} \sum_{q\nu} \sqrt{\frac{\hbar(n_{q\nu} + 1)}{m_b \omega_{q\nu}}} \cos(2\pi\eta_{1,q\nu}) \times \sqrt{-\ln(1 - \eta_{2,q\nu})} \tilde{e}_{b,q\nu}^\alpha e^{iq \cdot r_{bl}}, \quad (2)$$

where $u_{b,l}^\alpha$ is the thermal displacement of atom b in the l th unit-cell in the α -direction from its equilibrium position r_{bl} , m_b is the mass of atom b in the unit-cell, $n_{q\nu}$ is the Bose-Einstein distribution corresponding to temperature T , \hbar is the reduced Planck constant, $\omega_{q\nu}$ and $e_{q\nu}$ are phonon vibration frequency and eigenvector, and $\eta_{1,q\nu}$ and $\eta_{2,q\nu}$ are random numbers sampled from a uniform distribution and constrained by $\eta_{1,q\nu} = \eta_{1,-q\nu}$ and $\eta_{2,q\nu} = \eta_{2,-q\nu}$. The forces, F_i^α , acting on these thermally perturbed computational cells relate to potential energy, U , as

$$F_i^\alpha = -\frac{\partial U}{\partial u_i^\alpha}, \quad (3)$$

and U can be expanded using the Taylor series as

$$U = U_0 + \sum_i \Pi_i^\alpha u_i^\alpha + \frac{1}{2!} \sum_{ij} \Phi_{ij}^{\alpha\beta} u_i^\alpha u_j^\beta + \frac{1}{3!} \sum_{ijk} \Psi_{ijk}^{\alpha\beta\gamma} u_i^\alpha u_j^\beta u_k^\gamma + \frac{1}{4!} \sum_{ijkl} \Xi_{ijkl}^{\alpha\beta\gamma\delta} u_i^\alpha u_j^\beta u_k^\gamma u_l^\delta + O(u^5), \quad (4)$$

with $\Phi_{ij}^{\alpha\beta}$, $\Psi_{ijk}^{\alpha\beta\gamma}$, and $\Xi_{ijkl}^{\alpha\beta\gamma\delta}$ representing the harmonic, cubic, and quartic interatomic force constants. Thus, the finite-difference method can be used to obtain harmonic force constants and phonon eigenspectrum to generate thermally populated computational cells via Eq. (2). The forces obtained on these thermally populated cells can be employed to do force-displacement dataset fitting via Eqs. (3) and (4) to extract the cubic and quartic force constants (after removing the contribution of harmonic force constants from the forces). The force constants obtained using this process [labeled as thermal snapshot (TS)] are temperature-dependent.

Finally, instead of using Eq. (2), the thermally populated computational cells can be sampled from molecular dynamics simulations, and the resulting force-displacement dataset can again be fitted using Eqs. (3) and (4) to extract the desired force constants. The force constants obtained using this method are labeled as molecular dynamics (MD) and are temperature-dependent.

It is worthwhile to emphasize that in MD methodology, the force constants are extracted from the actual molecular dynamics simulations trajectories which does not allow over-/under-stretching of interatomic bonds. As such, large out-of-plane displacements of atoms from their equilibrium planar positions (rippling) are obtained only in relatively large graphene flakes (consisting of

>100–1000 unitcells). In the TS method, however, the atomic displacements are obtained by summing over all eigenmodes. As such, the rippling is possible even in relatively small unitcells if the contribution of flexural (rippling) modes is dominant.

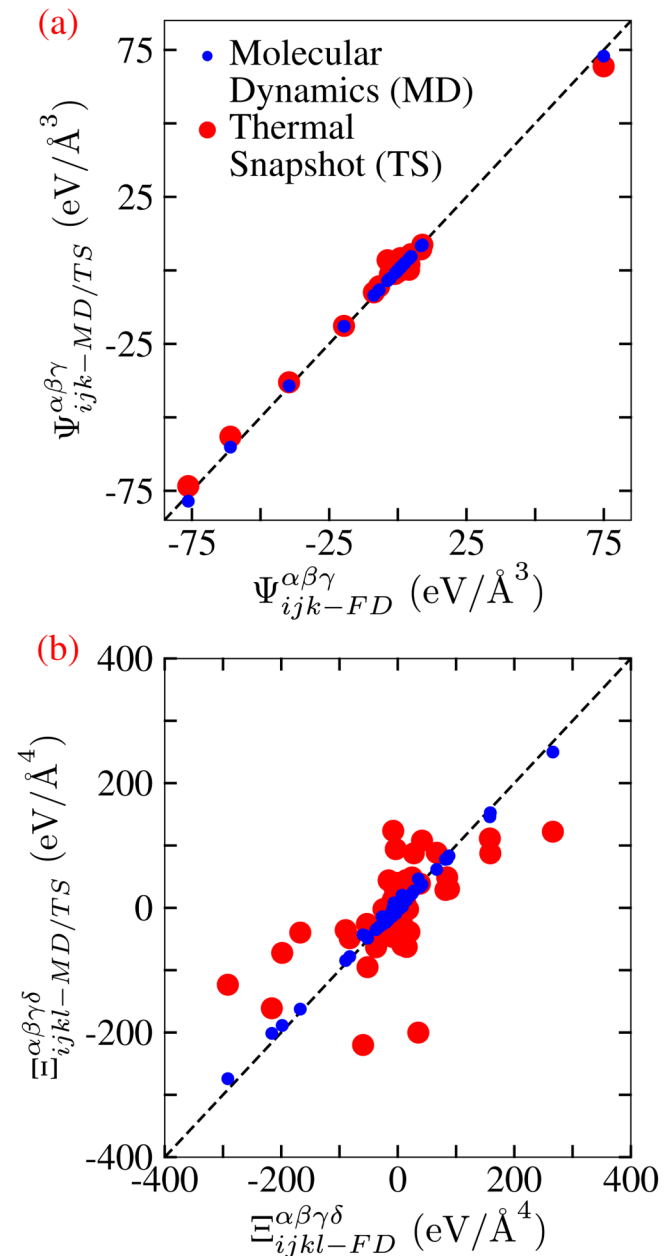


FIG. 2. The comparison of (a) cubic and (b) quartic IFCs as obtained from MD and TS approaches against those from the FD approach for single-layer graphene. Only unique (symmetry-unrelated) IFCs are included. The extracted cubic IFCs are similar from all approaches, and while the extracted quartic IFCs are still similar from MD and FD approaches, they are scattered from the TS approach.

Downloaded from http://pubs.aip.org/jap/article-pdf/doi/10.1063/5.0152112/1792241/3/215102_1_5.0152112.pdf

III. COMPUTATIONAL DETAILS

To stay consistent with previous literature studies, we employed optimized Tersoff potential to determine interatomic interactions in graphene.⁶ Unless specified otherwise, the force constants are extracted using 288 atom computational cells obtained from $12 \times 12 \times 1$ repetition of the two atoms primitive cell. The interaction cutoffs are set to 2nd nearest neighbor shell for all force constants (note that all interactions are zero beyond the 2nd nearest neighbor shell for the Tersoff interatomic potential). For the calculation of force constants using the FD method, one or more atoms are displaced by 0.0025 Å from their equilibrium positions in the required directions. For TS and MD methods, 100 thermal configurations are employed, resulting in 43 200 force-displacement equations for 175 symmetry-unrelated unknown force constants. For the MD method, the molecular dynamics simulations are performed using LAMMPS package²⁰ with a time step of 1 fs, where starting with the relaxed structure, atoms are initially allowed to equilibrate at 300K using the NVT ensemble for 1×10^6 time steps. Subsequently, atoms are allowed to evolve

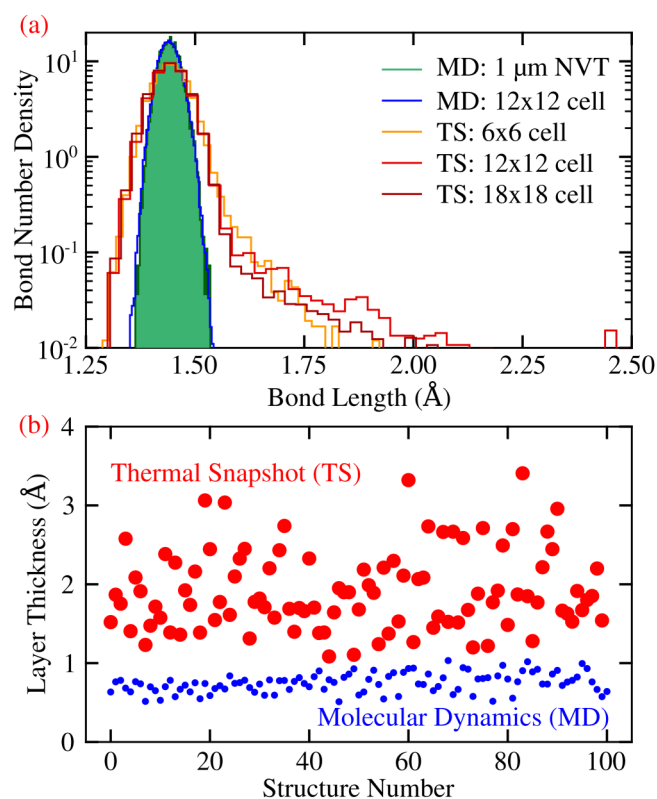


FIG. 3. The distribution of (a) interatomic bond lengths and (b) layer thickness in supercells obtained using the thermal snapshot and molecular dynamics approaches. The bond length distribution as obtained from molecular dynamics simulations of 1 μm graphene flake (with ripples) is also included in (a) in green for comparison. Due to the decoupling of flexural and basal-plane modes, the bond lengths range up to 2.5 Å from the TS approach.

under the NVE ensemble for another 1×10^6 time steps, and structural snapshots are dumped every 5000 steps. The phonon scattering rates are obtained using the phonon wavevector grid of size $40 \times 40 \times 1$ (same as that employed in Refs. 12 and 13), and the energy conservation delta functions in the calculation of phonon scattering rates are replaced by Gaussians with scattering-process dependent adaptive broadening as described in Ref. 21. The layer thickness of graphene is taken as 3.4 Å, and all reported results are for a temperature of 300 K.

For bi-layer graphene and bulk-graphite, the interlayer interactions are described using the Lennard-Jones interaction.²² The phonon scattering rates are obtained using wavevector grids of size $28 \times 28 \times 1$ and $12 \times 12 \times 10$ for bi-layer graphene and graphite, respectively. These grids result in a similar number of wavevector-atoms as that in $40 \times 40 \times 1$ grid single-layer graphene. The thermal conductivity obtained using the RTA solution of BTE with only three-phonon scattering varies by less than 15% in increasing the phonon wavevector grid from $12 \times 12 \times 10$ to $24 \times 24 \times 16$ for graphite.

For obtaining bond lengths from molecular dynamics simulations, we employed the non-equilibrium method by applying a small temperature difference (60 K) across the 1 μm length sample. The sample is subjected to periodic boundary condition in the perpendicular direction. We started with a 0 K structure and heated the structure to 300 K for 500 ps using a time step of 0.5 fs in the NPT ensemble. Subsequently, the two ends of the sample are maintained at 330 and 270 K using the Nosé-Hoover thermostats, and the system is allowed to equilibrate under the NVT ensemble for 3000 ps. Finally, the simulation is run for additional 6 000 000 time steps during which bond lengths are sampled from the central region with linear temperature profile. We note that we used molecular dynamics simulations only to sample the interatomic bond lengths and force constants, i.e., we do not report any thermal conductivity obtained directly using molecular dynamics simulations.

IV. RESULTS

The thermal conductivity of isotopically pure single-layer graphene as obtained using different force constants extraction methodologies using relaxation time approximation (RTA) solution of the BTE is reported in Fig. 1(a). Using the FD approach, we obtain thermal conductivity of 315 W/m K, which is in close agreement with that reported by Feng and Ruan.¹² In our calculations, we approximated energy conservation delta functions by Gaussians with adaptive broadening,²³ and we find that thermal conductivity changes by less than 5% on scaling the employed broadening amount by a factor of 5. The change is more when the broadening function is replaced by Lorentzians of similar widths but is less than 15% for all considered cases.

When the temperature-dependent force constants as obtained using the thermal snapshot technique are used, the thermal conductivity increases by more than a factor of 3 in comparison to the value from the finite-difference approach, which is consistent with the results of Gu *et al.*¹³ However, the obtained thermal conductivity is not converged and varies drastically with the size of the computational cell employed to extract the force constants. This is

despite ensuring over-specified systems with at least 100 times more equations than the number of unknown force constants. In contrast, when molecular dynamics simulations based force constants are used, the obtained thermal conductivity is converged and is within 3% of that obtained from the finite-difference method.

To understand the origin of this over-prediction and non-convergence of thermal conductivity by the thermal snapshot technique, we plot the bare cubic and quartic, symmetry-unrelated force constants as obtained using different methodologies in Fig. 2. We find that the cubic and quartic force constants obtained from the molecular dynamics simulation data are similar to those obtained using the finite-difference method. For the thermal snapshot technique, while the cubic force constants are still similar to those obtained using the finite-difference method, the quartic counterparts are more scattered and are highly dependent on the computational supercell size. We hypothesize that this scattering of quartic force constants via the thermal snapshot technique is an outcome of the over-stretching of bonds owing to weak vibration frequencies of flexural modes [see Eq. (2)]. We tested this by plotting the distribution of bond lengths as obtained via the thermal snapshot technique and molecular dynamics-based methods in Fig. 3(a) (for the finite-difference based method, all bond lengths are fixed at 1.44 Å).²⁴ For comparison, we also sampled bond lengths from molecular dynamics simulations on 1 μm length

sample subjected to NVT ensemble at 300 K, which has large ripples.

We find that the bond lengths in molecular dynamics trajectories range up to 1.5 Å. For the thermal snapshot technique, the range is much larger, with bonds stretching up to 2.5 Å. This over-stretching of bonds via the thermal snapshot technique is non-physical and is due to the failure of the thermal snapshot technique for decoupled flexural and basal-plane modes, as is the case for graphene. In particular, the thermal displacements of atoms via Eq. (2) (which are obtained by summing over all modes) are decoupled in the flexural and basal-plane directions. Owing to weak vibration frequencies of flexural modes, the obtained thermal displacements are large in the cross-plane direction (independent of in-plane direction), thus resulting in excessive bond stretching. This is confirmed in Fig. 3(b) where the thickness of $12 \times 12 \times 1$ graphene sheets is reported and is found to vary between 1 and 3 Å for thermal snapshot-based configurations as opposed to 0.5–1 Å in molecular dynamics simulations.

For single-layer graphene, since the thermal snapshot method results in non-physical bond lengths, we predicted thermal conductivity only using the finite-difference based force constants. Using the iterative solution of the BTE, our predicted thermal conductivity is 796 W/mK, which agrees with the value of 810 W/mK reported by Feng and Ruan¹² using the same approach. However, this value is a severe under-prediction of experimentally measured values.^{1–3,5,16}

To test, if this under-prediction of thermal conductivity is due to phonon renormalization, we used (i) real space harmonic force constant renormalization based on quartic force constants (corresponding to infinite summation of loop diagrams)⁹ and (ii) bubble and loop shifts based on Dyson's approach.²³ We find that while the thermal conductivity increases with both approaches, the change is less than 25% [Fig. 1(a)], which is insufficient in explaining the factor of three-five difference in the BTE predicted thermal conductivity as compared to the experimental measurements.

While the above analysis establishes that the thermal snapshot technique-based interatomic force constants are non-physical for single-layer graphene, its applicability for bi/multi-layer graphene and graphite is also unclear. To test for this, we report the distribution of interatomic bond lengths as obtained using the thermal snapshot technique-based snapshots for bi-layer graphene and graphite in Fig. 4(a). We find that the bond lengths vary only up to 1.6 Å in bi-layer graphene and graphite using the thermal snapshot technique though the variation is up to 2.5 Å in graphene using the same technique. Further, the obtained temperature-dependent cubic and quartic interatomic force constants from thermal snapshot technique are similar to those obtained using the finite-difference approach [see Figs. 4(b) and 4(c)], thus suggesting the negligible effect of temperature-dependent force constants on the predicted thermal conductivity.

For bi-layer graphene, the effect of temperature-dependent force constants is significant and the thermal conductivity increases by more than 25% with thermal snapshot based force constants using the RTA solution of the BTE and three-phonon scattering [Fig. 5(a)]. For graphite, temperature has negligible effect on force constants and the predicted difference in thermal conductivity is less than 5% when thermal snapshot approach is used opposed to

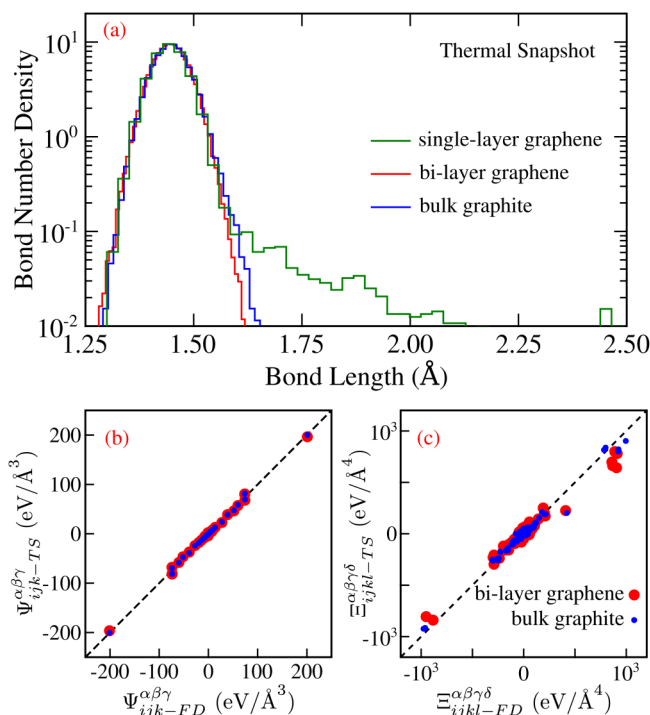


FIG. 4. (a) The distribution of interatomic bond lengths in supercells obtained using the thermal snapshot approach for single- and bi-layer graphene and graphite. The comparison of (b) cubic and (c) quartic IFCs as obtained from the TS approach against those from the FD approach.

the finite-difference approach for the extraction of force constants. This is consistent with relatively large thermal mean square displacements of atoms in the flexural direction for bi-layer graphene compared to that in graphite (0.04 \AA^2 for bi-layer graphene compared to 0.01 \AA^2 for graphite).

For both bi-layer graphene and graphite, the four-phonon scattering has a little effect on the thermal conductivity and the obtained thermal conductivity decreases by less than 10% using the RTA solution of the BTE and thermal snapshot technique-based force constants [Fig. 5(a)]. With iterative solution of the BTE, the obtained thermal conductivities are 2700 and 2000 W/mK for bi-layer graphene and graphite. Note that these thermal conductivities are obtained without considering phonon-isotope scattering and is expected to decrease by 10%–15% for naturally occurring samples with C-13 isotopes, thereby bringing the final thermal conductivities in excellent agreement with the literature.²⁵

V. DISCUSSION

The BTE method is a very powerful tool to predict the thermal conductivity of materials. The accuracy of predicted thermal conductivity depends on the interatomic force constants. In the particular case of single-layer graphene, due to the presence of low-frequency flexural modes, the atoms are displaced from their 0 K equilibrium planar positions by more than a few \AA at non-zero temperatures. Because of such large displacements of atoms from their 0 K equilibrium position, it is necessary to include temperature-dependence effects in the extraction of force

constants. This is indeed observed by Gu *et al.*¹³ where the thermal conductivity was found to increase significantly with temperature-dependent force constants for single-layer graphene in comparison to results presented by Feng and Ruan.¹² The employed methodology for the extraction of temperature-dependent force constants by Gu *et al.* is, however, thermal snapshot technique which results in an over stretching of interatomic C–C bonds to 2–3 \AA for single layer graphene and is, therefore, non-physical. Further, the force constants are extracted using the Taylor-series force-displacement data-fitting in thermal snapshot technique, which itself is questionable for large atomic displacements of a few \AA . Both of these concerns are potentially addressable by using a large unitcell in BTE calculations where the equilibrium positions of atoms is rippled/displaced structure and interatomic force constants are extracted about these rippled/displaced equilibrium positions. However, such unitcell will have several hundred atoms to correctly capture the rippled structure and is beyond the scope of currently available computational resources. As such, it is not possible to conclude the effect of temperature-dependent force constants on the predicted thermal conductivity of single layer graphene via the BTE method using current computational resources. Finally, we emphasize that the obtained non-physical description of interatomic bonds via the TS method is due to decoupled basal-/flexural modes with quadratic dispersion in graphene. Since these characteristic are due to planar structure of graphene, they are expected to be present for all planar materials (such as flat hexagonal boron nitride) independent of the employed interatomic interaction approach (density functional theory vs empirical forcefields).

VI. CONCLUSIONS

To summarize, the thermal conductivities of single-/bi-layer graphene and graphite are obtained by considering the three-phonon and four-phonon scatterings in the Boltzmann transport equation (BTE) framework with temperature-independent and temperature-dependent interatomic force constants. While the temperature-independent finite-difference based force constants result in a correct description of interatomic distances, they are not able to capture the rippled non-planar structure of single-layer graphene at non-zero temperatures and results in a severe under-prediction of experimentally measured thermal conductivity. On the other hand, while the thermal snapshot technique for temperature-dependent force constant extraction results in rippled structures for single-layer graphene, the obtained C–C bond lengths are non-physical. The correct description of temperature-dependent force constants via the thermal snapshot technique requires much larger non-planar/rippled unitcells for single-layer graphene, for which thermal conductivity predictions via BTE are not possible using current computational resources. As such, the literature reports on the effect of temperature on interatomic force constants of single layer graphene require further consideration.

ACKNOWLEDGMENTS

The authors acknowledge the financial support from the National Supercomputing Mission, Government of India (Grant No. DST/NSM/R&D-HPC-Applications/2021/10) and Core Research Grant, Science & Engineering Research Board, India

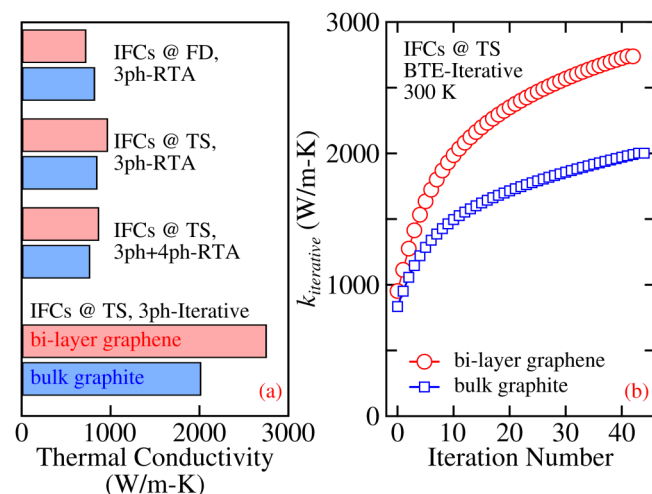


FIG. 5. The effect of (a) temperature-dependent force constants, four-phonon scattering, and (b) iterative solution of the BTE on the predicted thermal conductivity of bi-layer graphene (red) and bulk-graphite (blue). The thermal conductivity reduces by less than 10% for both bi-layer graphene and graphite with four-phonon scattering using the RTA solution of the BTE. While the use of temperature-dependent IFCs using TS method results in less than 5% change in the thermal conductivity of graphite, the thermal conductivity of bi-layer graphene increases by more than 25% with temperature-dependent IFCs using the RTA solution of the BTE.

(Grant No. CRG/2021/000010). The calculations are carried out on SpaceTime-II supercomputing facility of IIT Bombay and PARAM Sanganak supercomputing facility of IIT Kanpur.

AUTHOR DECLARATIONS

Conflict of Interest

The authors have no conflicts to disclose.

Author Contributions

Shadab Alam: Formal analysis (equal); Methodology (equal); Validation (equal); Visualization (equal); Writing – original draft (equal). **Amey G. Gokhale:** Formal analysis (equal); Investigation (equal); Methodology (equal); Validation (equal); Visualization (equal); Writing – original draft (equal). **Ankit Jain:** Conceptualization (lead); Formal analysis (equal); Funding acquisition (lead); Investigation (equal); Methodology (equal); Project administration (lead); Resources (lead); Supervision (lead); Validation (equal); Writing – review & editing (equal).

DATA AVAILABILITY

The data that support the findings of this study are available from the corresponding author upon reasonable request.

REFERENCES

- ¹A. A. Balandin, “Thermal properties of graphene and nanostructured carbon materials,” *Nat. Mater.* **10**, 569–581 (2011).
- ²W. Cai, A. L. Moore, Y. Zhu, X. Li, S. Chen, L. Shi, and R. S. Ruoff, “Thermal transport in suspended and supported monolayer graphene grown by chemical vapor deposition,” *Nano Lett.* **10**(5), 1645–1651 (2010).
- ³S. Chen, A. L. Moore, W. Cai, J. W. Suk, J. An, C. Mishra, C. Amos, C. W. Magnuson, J. Kang, L. Shi, and R. S. Ruoff, “Raman measurements of thermal transport in suspended monolayer graphene of variable sizes in vacuum and gaseous environments,” *ACS Nano* **5**(1), 321–328 (2011).
- ⁴J. H. Seol, I. Jo, A. L. Moore, L. Lindsay, Z. H. Aitken, M. T. Pettes, X. Li, Z. Yao, R. Huang, D. Broido, N. Mingo, R. S. Ruoff, and L. Shi, “Two-dimensional phonon transport in supported graphene,” *Science* **328**(5975), 213–216 (2010).
- ⁵S. Chen, Q. Wu, C. Mishra, J. Kang, H. Zhang, K. Cho, W. Cai, A. A. Balandin, and R. S. Ruoff, “Thermal conductivity of isotopically modified graphene,” *Nat. Mater.* **11**(3), 203–207 (2012).
- ⁶L. Lindsay, D. A. Broido, and N. Mingo, “Flexural phonons and thermal transport in graphene,” *Phys. Rev. B* **82**, 115427 (2010).
- ⁷L. Lindsay, W. Li, J. Carrete, N. Mingo, D. A. Broido, and T. L. Reinecke, “Phonon thermal transport in strained and unstrained graphene from first principles,” *Phys. Rev. B* **89**, 155426 (2014).
- ⁸A. Jain, “Multichannel thermal transport in crystalline Ti_3VSe_4 ,” *Phys. Rev. B* **102**(20), 201201 (2020).
- ⁹A. Jain, “Single-channel or multichannel thermal transport: Effect of higher-order anharmonic corrections on the predicted phonon thermal transport properties of semiconductors,” *Phys. Rev. B* **106**, 045207 (2022).
- ¹⁰N. K. Ravichandran and D. Broido, “Unified first-principles theory of thermal properties of insulators,” *Phys. Rev. B* **98**(8), 085205 (2018).
- ¹¹Y. Xia, K. Pal, J. He, V. Ozoliņš, and C. Wolverton, “Particlelike phonon propagation dominates ultralow lattice thermal conductivity in crystalline Ti_3VSe_4 ,” *Phys. Rev. Lett.* **124**(6), 065901 (2020).
- ¹²T. Feng and X. Ruan, “Four-phonon scattering reduces intrinsic thermal conductivity of graphene and the contributions from flexural phonons,” *Phys. Rev. B* **97**(4), 045202 (2018).
- ¹³X. Gu, Z. Fan, H. Bao, and C. Y. Zhao, “Revisiting phonon-phonon scattering in single-layer graphene,” *Phys. Rev. B* **100**(6), 064306 (2019).
- ¹⁴O. Hellman, P. Steneteg, I. A. Abrikosov, and S. I. Simak, “Temperature dependent effective potential method for accurate free energy calculations of solids,” *Phys. Rev. B* **87**(10), 104111 (2013).
- ¹⁵V. K. Tewary and B. Yang, “Singular behavior of the Debye-Waller factor of graphene,” *Phys. Rev. B* **79**(12), 125416 (2009).
- ¹⁶A. H. Castro Neto, F. Guinea, N. M. R. Peres, K. S. Novoselov, and A. K. Geim, “The electronic properties of graphene,” *Rev. Mod. Phys.* **81**, 109–162 (2009).
- ¹⁷A. J. H. McGaughey, A. Jain, H.-Y. Kim, and B. Fu, “Phonon properties and thermal conductivity from first principles, lattice dynamics, and the Boltzmann transport equation,” *J. Appl. Phys.* **125**(1), 011101 (2019).
- ¹⁸N. Shulumba, O. Hellman, and A. J. Minnich, “Intrinsic localized mode and low thermal conductivity of PbSe,” *Phys. Rev. B* **95**(1), 014302 (2017).
- ¹⁹D. West and S. K. Estreicher, “First-principles calculations of vibrational lifetimes and decay channels: Hydrogen-related modes in Si,” *Phys. Rev. Lett.* **96**(11), 115504 (2006).
- ²⁰A. P. Thompson, H. M. Aktulga, R. Berger, D. S. Bolintineanu, W. M. Brown, P. S. Crozier, P. J. in ’t Veld, A. Kohlmeyer, S. G. Moore, T. D. Nguyen, R. Shan, M. J. Stevens, J. Tranchida, C. Trott, and S. J. Plimpton, “LAMMPS—A flexible simulation tool for particle-based materials modeling at the atomic, meso, and continuum scales,” *Comp. Phys. Comm.* **271**, 108171 (2022).
- ²¹J. R. Yates, X. Wang, D. Vanderbilt, and I. Souza, “Spectral and Fermi surface properties from Wannier interpolation,” *Phys. Rev. B* **75**(19), 195121 (2007).
- ²²X. Wang, Y. Hong, D. Ma, and J. Zhang, “Molecular dynamics study of thermal transport in a nitrogenated holey graphene bilayer,” *J. Mater. Chem. C* **5**(21), 5119–5127 (2017).
- ²³J. E. Turney, E. S. Landry, A. J. H. McGaughey, and C. H. Amon, “Predicting phonon properties and thermal conductivity from anharmonic lattice dynamics calculations and molecular dynamics simulations,” *Phys. Rev. B* **79**, 064301 (2009).
- ²⁴Note that the interatomic bond lengths and layer thickness as reported in Fig. 3 are obtained after the first iteration of the TS method. Due to large atomic displacements of atoms from the equilibrium positions, the validity of Taylor-series fitting to force–displacement dataset via Eq. (3) is questionable and as such, subsequent iterations are not performed.
- ²⁵L. Lindsay, D. A. Broido, and N. Mingo, “Flexural phonons and thermal transport in multilayer graphene and graphite,” *Phys. Rev. B* **83**(23), 235428 (2011).